International Journal of Thermofluids 9 (2021) 100068

Contents lists available at ScienceDirect

International Journal of Thermofluids

journal homepage: www.elsevier.com/locate/ijtf

Experimental and analytical study of open pore cellular foam material on the performance of proton exchange membrane electrolysers

F.N. Khatib[a], Tabbi Wilberforce[b,*], James Thompson[a], A.G. Olabi[b,c]

[a] Institute of Engineering and Energy Technologies, University of the West of Scotland, Paisley, United Kingdom
[b] Mechanical Engineering and Design, School of Engineering and Applied Science, Aston University, Aston Triangle, Birmingham B4 7ET, United Kingdom
[c] Department of Sustainable and Renewable Energy Engineering, University of Sharjah, Sharjah, United Arab Emirates

ARTICLE INFO

Article History:
Received 15 August 2020
Revised 24 January 2021
Accepted 2 February 2021
Available online 7 February 2021

Keywords:
PEM electrolysers
Computational fluid dynamics
Polarisation curve
Open pore cellular foam material

ABSTRACT

The aim of this research is to develop research methodology and provide insight into the viability of using Open Pore Cellular Foam (OPCF) material in Polymer Electrolyte Membrane (PEM) Electrolysers. Analysis have therefore been carried out on three different types of electrolyser geometries. A PEM electrolyser is considered with serpentine, mesh and OPCF flow channels, whilst all the other physical and operational parameters are kept constant. Three dimensional models have been created in solid works and computational fluid dynamic simulations have been carried out on all the three types of electrolysers in ANSYS Fluent. Experimental investigations have also been carried out using all the three different flow plate geometries. ANSYS simulation show that the performance of the OPCF flow channel electrolyser is 1.5 times higher than that of the mesh channel electrolyser. Experimental results have shown that using OPCF flow channel the performance of the electrolyser improves significantly by 17% to that compared with conventional mesh flow plate electrolysers.

1. Introduction

Scientists around the world today are considering alternative form of energy generation. This is because the main source of power generation (fossil fuel/commodities) have been scientifically proven to have harsh effect on the environment [1–3]. Again, prices of fossil products are unstable. Researchers in recent times have considered renewable energy as alternative to fossil fuel as it is friendly to the environment, considered to be sustainable and abundant [4,5]. Countries around the world are making huge investment into this sector. Storage of the energy generated from renewable sources remain a challenge. Energy from renewable sources are intermittent and fluctuate hence their storage is very vital. The excess electricity from renewable sources when demand is low can be used in splitting water for hydrogen production. The stored hydrogen with the aid of an energy converting device like fuel cell can produce electricity when energy demand is high hence making electrolysers suitable for energy management [6–9]. Today several research activities are being championed in this grey area because hydrogen does not function in their molecular structure [10–12]. To generate hydrogen, there must be an energy input. Steam reforming of natural gas is a well-known process for generation of hydrogen [13]. Apart from producing hydrogen from propane, gasoline, diesel, methanol or ethanol via steam reforming [14–15], hydrogen is considered as one of the best vectors/carriers for storing renewable and intermittent energy from sources including wind and solar, or off-peak energy from the grid [16–18]. The methodology for steam reforming is to react fossil fuel with steam in the form of water vapour at high temperatures between 700 - 1100 °C in a device called the reformer. Nickel is used as a catalyst to speed up the chemical reaction in the reformer. The hydrogen produced by steam reforming are of low purity with some concentration of carbon-based species like carbon monoxide. Hydrogen produced from steam reforming still has immense impact on the environment and does not in any way reduce the high dependency on fossil commodities with limited reserves. Production of hydrogen can be accomplished by splitting water into hydrogen and oxygen electrochemically. The process is called water electrolysis as shown in Eq. (1).

$$H_2O_{(l)} + 237.2kJmol^{-1} + 48.6kJmol^{-1} \rightarrow H_2 + 1/2O_2 \quad (1)$$

The design of the PEM electrolyser [19] is another critical aspect of the hydrogen generation process that determines the purity as well as the amount of hydrogen generated. Fuel cells which are often used in conjunction with electrolysers generates electricity via a reaction between the hydrogen produced by the electrolyser and air(oxidant) with water and heat being the end product [20–30]. This

* Corresponding author.
E-mail address: t.awotwe@aston.ac.uk (T. Wilberforce).

https://doi.org/10.1016/j.ijft.2021.100068

Nomenclature

AC	Alternating current
CNLS	Complex non-linear least square
EEC	Electrical equivalent circuit
EIS	Electrochemical impedance spectroscopy
MEA	Membrane electrode assembly
OPCF	Open pore cellular foam
PEM	Polymer electrolyte membrane
PEMEL	Polymer electrolyte membrane electrolyser
PEMWE	Polymer electrolyte membrane water electrolysis
UC	Unit Cell
WE	Water electrolysis

investigation will therefore explore experimentally and analytically the performance of a PEM electrolyser using open pore cellular foam material as the flow channel.

2. Experimental set up

The PEM electrolyser is set up according to a commonly used PEM electrolyser configuration consisting of a membrane electrode assembly (MEA); gas diffusion layers (GDLs) and bipolar plates (BPs) with flow channels. Fig. 1 shows the balance of plant of the PEM water electrolysis system used in this experiment for control and measurement. This single-cell electrolyser was designed for an active area of 115 cm^2. The water bath was set at a desired experimental temperature which was controlled remotely by switching the heater on and off by external control. De-ionized water was supplied for electrolysis. The water flow rate was controlled by pulse wave modulation (PWM) of the motor. A total of 3 experiments were carried out to determine an informed estimate of the flow rate. A programmable DC supply Agilent® 3660 was used as a power source to electrolyse water into hydrogen and oxygen. The thermocouples in the system aided in the measurement of the cell temperature. All data were controlled and recorded in real time by LabVIEW data acquisition system. External circuit using the Arduino Mega 2560 was used to provide interface between PC and the electrolyser balance of plant (BOP). The effect of the velocity of the circulating liquid water on the electrolyser performance and pressure drop was evaluated for electrolyser using three different types of flow fields (a) a single channel serpentine flow field, (b) Mesh flow field and (c) OPCFM flow field. The flow field of both electrode sides was the same.

3. Design of 3D PEM electrolyser models

In order to investigate the performance of electrolyser using ANSYS flow simulation, a PEM electrolyser needs to be modelled with all the

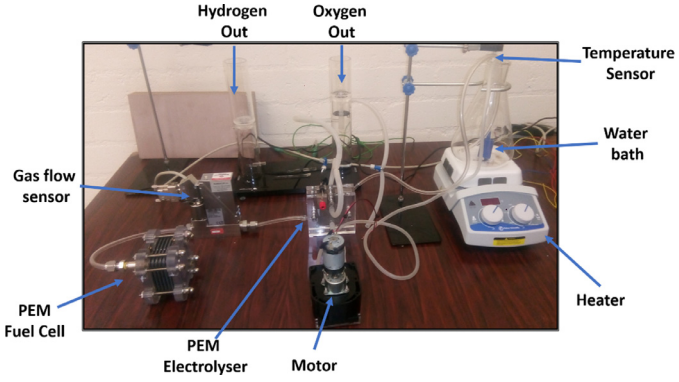

Fig. 1. PEM electrolyser experimental setup.

9 layers of the electrolyser. A total of three, 3D models were created with different flow channel orientations of serpentine flow channel, Mesh flow channel and the OPCF flow channel as shown in Fig. 2.

Fig. 2 shows the layout of a 3D modelled PEM electrolyser along with its distinguished 9 layers. In order to investigate the effect of the flow channel on the performance of the electrolyser, the design of the electrolyser had to be made 'fit for all' so that all the other factors are constant and only the flow channel needs to be redesigned. In doing so, the current collectors, gasket, MEA all were kept to constant dimensions. Fig. 3 shows the current collector design. The dimensions of which are kept in 'cm' scale and it was aimed that the active area of the current collector, is that of the MEA, which for the purpose of simulation was fixed approximately at 115cm^2.

Fig. 4 shows the bipolar plate design for the serpentine channel. The thickness of the serpentine channel was 0.2 mm while the bipolar plate hand a land width of 1 mm. This was considered as being defined as one of the optimum land widths for serpentine channel fuel cells in [6].

Fig. 5 shows a 3D view of the Membrane Electrode Assembly along with the 5 layers of the MEA. Electrolyser MEA's widely used in the industry are the catalyst coated Nafion membranes which comprise of 3 layers. The ANSYS fuel cell and electrolyser module needs an MEA designed such that it consists of 2 gas diffusion layers, 2 catalyst layers and 1 membrane layer as shown in Fig. 5. Since membrane dynamics was not the area of this research, a 5 layer MEA was therefore modelled as shown in Fig. 5(b). Fig. 6 shows the gasket design used. It is an essential part of the design which electrically isolates the Anode side of the MEA to the Cathode side.

As discussed earlier, the aim is to evaluate the effect of geometry design on the performance of a PEM electrolyser with different flow channels. In doing so, every aspect of the design had been kept unchanged, but modelling had to be done for the mesh design. The mesh flow plate design as shown in Fig. 7 has the same active area of 115cm^2 as that of the serpentine flow plate.

High porosity open-cell metal foams typically have stochastic cellular morphology, as shown in Fig. 8. To directly model the effect of an OPCF material flow channel in PEM electrolyser, the full size of the block had to be considered. To simplify the problem, two fundamental assumptions were considered;

1) It as was assumed that the metallic matrix is periodic
2) To employ tetrakaidekahedron unit cell (UC) to represent the real foam topology.

Fig. 8 presents the reconstructed tetrakaidekahedron cells, which was centrally cut by a sphere of 5.08 mm in diameter, resulting in a pore density of 5 PPI (pores per inch). Correspondingly, the volume fraction (porosity) of the UC (or foam) was 0.90 [8].

The sphere-cut tetrakaidekahedron as shown in Fig. 9 consisted of six squares, internally cut by a sphere with diameter D1 eight hexagonal faces, internally cut by a sphere with diameter D2. Further the tetrakaidekahedron was centrally but by a sphere with diameter D3. With global size a and ligament length t, the porosity of the sphere cut tetrakaidekahedron were given by,

$$porosity = \frac{\pi}{4}\left[2\left(3+2\sqrt{3}\right)\left(\frac{D_3}{a}\right)^2 - 8\left(\frac{D_3}{a}\right)^3 - \left(2+\sqrt{3}\right)\right] \quad (2)$$

Fig. 10 shows the bipolar plate assembly for the Open pore cellular foam material channel. Section 4 will discuss and analyse simulation results for studied geometry which will provide the information to perform experimental investigation.

4. Results and discussions

As discussed earlier that the data acquisition and monitoring was carried out in LabVIEW, however, to achieve this an electronic

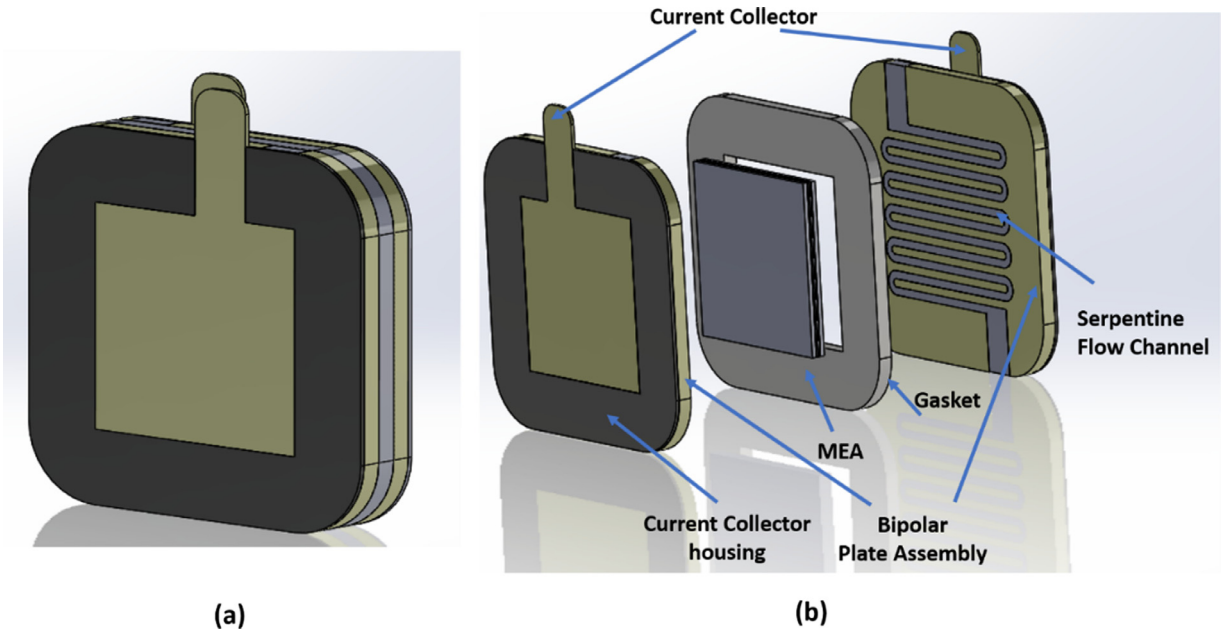

Fig. 2. (a) 3D model of a PEM Electrolyser (b) Exploded image of a PEM electrolyser with Serpentine flow plate channel.

interface between the electrolyser and the LabVIEW was required. The electronic interface was provided by designing a specific circuit that provided autonomous control as shown in Fig. 11. The interface board in Fig. 11 was designed to link the electrolyser and its auxiliaries to the LabVIEW interface so that timely data can be monitored and controlled. As part of the experimental procedure a balanced system was created such that the output of the generated gas from the electrolyser was connected to the fuel cell. The fuel cell load. The oxygen and hydrogen flows were measured in LabVIEW using Bronkhorst EL-Flow mass controller. Since the electrolyser current dictates, the amount of hydrogen being produced, the fuel cell load was therefore kept at 10% lower to that of the electrolyser driving current. This was done to provide a balanced system, and to generate a I-V or polarisation curve. The polarisation curve was generated using the data logged in the LabVIEW software.

4.1. Experimental results and discussions

To identify the performance of the electrolyser experimentally the electrolyser operating temperature was increased from 30 °C to 70 °C in 10 °C increments, and the pressure is fixed at 1 atm. The current density is measured for the temperature-dependant voltage change and generated hydrogen and oxygen flow rates. All the results presented is an average based on five experiments conducted repetitively. This approach therefore reduced the margin of error culminating from the measuring instrument used for the investigation. Fig. 12(a) – (c) shows the effect of the flow field on the PEM electrolyser polarization curves at various temperatures under atmospheric pressure.

It can be seen in all the graphs in Fig. 12, that the electrocatalytic activity increased as a function of temperature due to the activation behaviour of the irreversible O_2 evolution occurring at the IrO_2 electrocatalyst in the MEA. The best performance can be seen is obtained at 70 °C. The operation of the electrolyser was not studied at a higher temperature to avoid dehydrating the Nafion membrane and softening the gaskets.

The polarization curve is the core of the PEM electrolyser performance, which depends on the input current, the water temperature and some constitutive internal resistances. Fig. 13 compares the polarization curves obtained experimentally for the three different flow fields, serpentine, mesh and OPCF, at a cell temperature of 70 °C. When the cell temperature is 70 °C, the cell voltage for the OPCFM is the lowest compared to that of the other flow fields. From the graph, it can be seen that the voltage increases nonlinearly up to almost 0.05 A/cm^2 and linearly thereafter. The slope of this linear curve

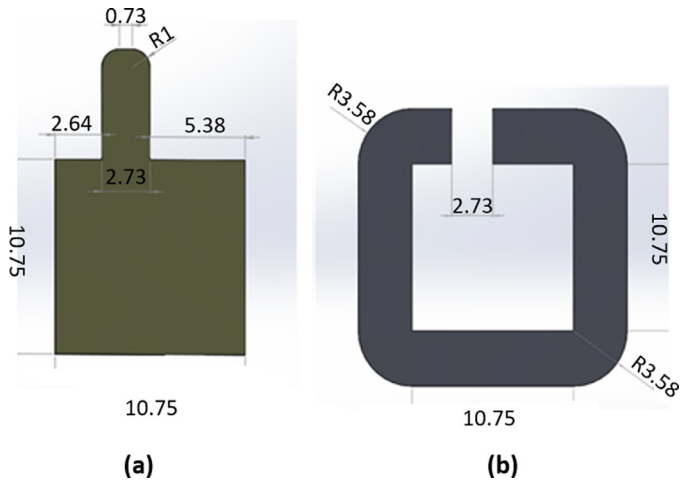

Fig. 3. (a) PEM electrolyser Current collector with active area of 115cm^2 (b) Current collector housing.

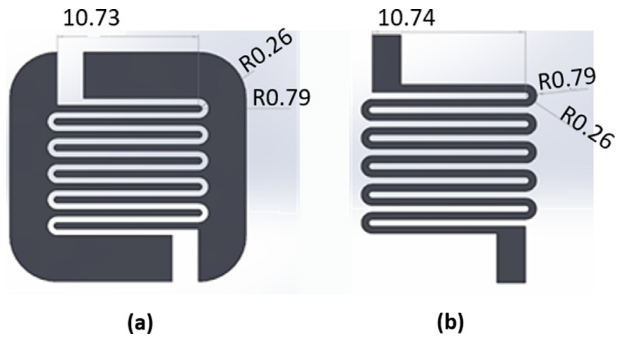

Fig. 4. PEM electrolyser Serpentine bipolar plate (b) Serpentine bipolar plate channel used for simulation and fluid flow analysis.

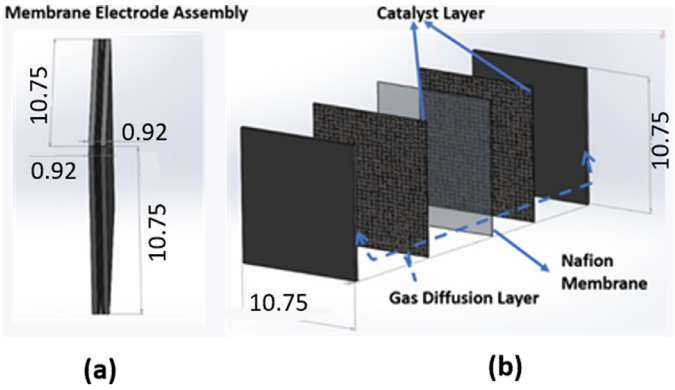

Fig. 5. (a) 3D Membrane Electrode Assembly (b) Schematic view of the 5 layers of an MEA.

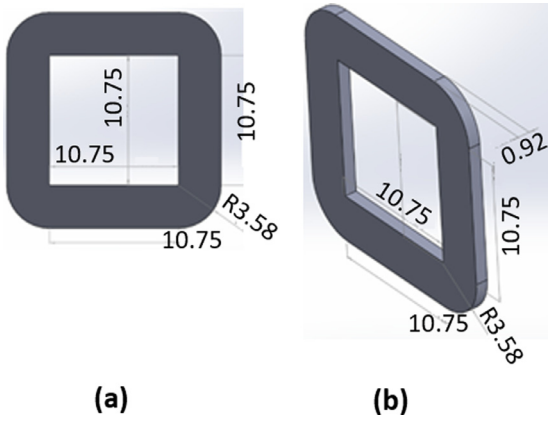

Fig. 6. (a) 3D Gasket model for the design.

represents the electrical resistances inside the cell. The ANSYS simulation results predicted the qualitative cell polarization curve; however, the measured voltage is higher than the analytical voltage due to internal electrical resistances. This higher performance in the PEM electrolyser for the PEM electrolyser with an OPCF flow channel is also due to the lower pressure drop offered by the channel as discussed earlier.

The experimental results show that using an OPCF flow plate (porous channel) outperformed the mesh and serpentine flow plate, recording 2.5 V at 1.4A/cm^2. This is in excess of approximately 17% improvement on the current density of the benchmark mesh flow plate under the same operating conditions operating at 2.5 V. The

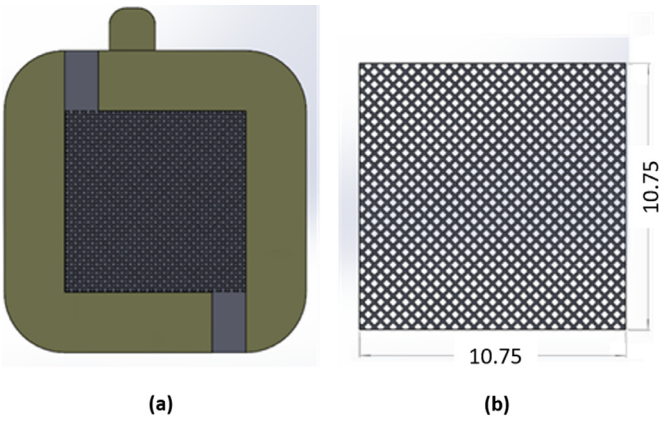

Fig. 7. (a) Mesh flow plate channel assembly (b) Mesh channel design.

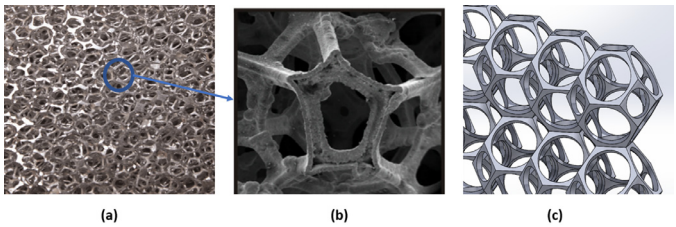

Fig. 8. (a) Aluminium metal foam (b) SEM image of a unit cell depicting a tetrakaidekahedron shape (c) OPCF flow channel assembly.

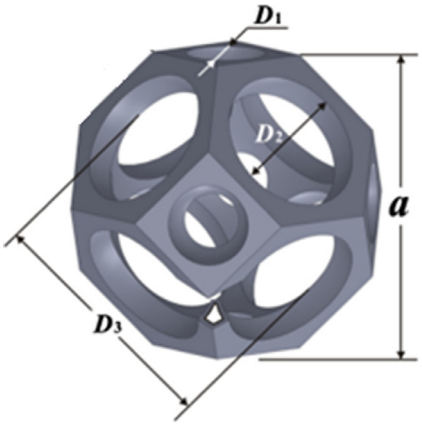

Fig. 9. Tetrakaidekahedron shape unit cell structure for Open pore cellular foam material.

overvoltage in the high-current-density region was larger when the flow velocity of the circulating water in the channel was higher because the flow rate per channel, and thus the flow velocity, is significantly different for various flow fields and depends on the type of flow field, even when the flow rate is the same. This finding suggests that an increase in overvoltage in the high current density region is caused by an increase in concentration overvoltage and suggests a relation between the flow velocity and the concentration overvoltage.

Electrochemical impedance spectroscopy (EIS) is a suitable and powerful diagnostic method for polymer electrolyte membrane water electrolysis cells (PEMWE) because it is non-destructive and provides useful information on performance and cell voltage losses associated with components. EIS measures the frequency dependence of the impedance, of a water electrolysis (WE) cell by applying a small alternating current (AC) in galvanostatic mode as a

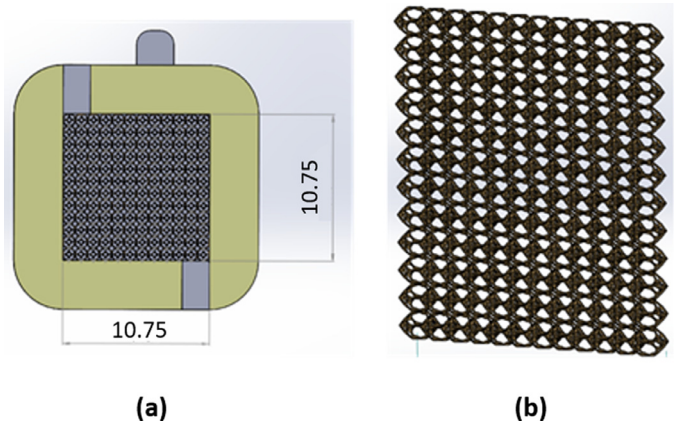

Fig. 10. (a) Bipolar plate assembly of OPCF material (b) Array of UCs forming the entire OPCF flow channel assembly.

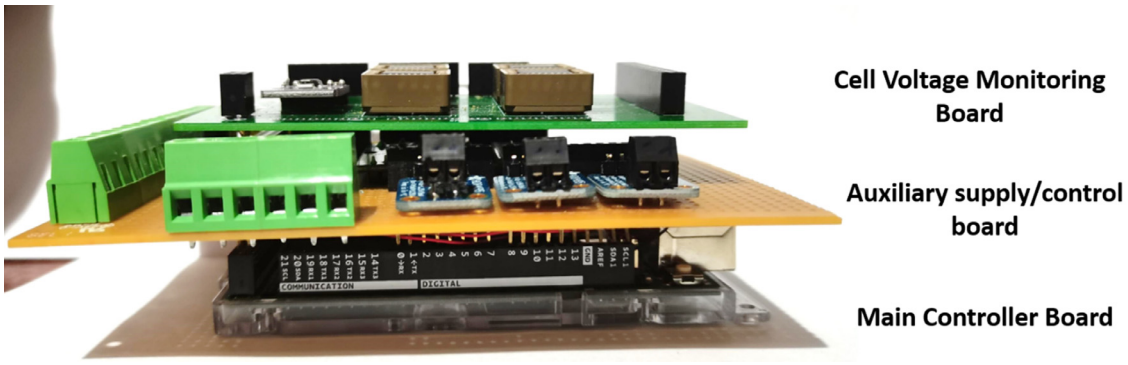

Fig. 11. Stacked control board with the bottom layer as the main controller, followed by the control board and the cell voltage monitoring board.

perturbation signal while measuring the alternating cell-voltage response. In potentiostatic mode, a small alternating voltage is applied and the AC response is measured.

The use of small (sinusoidal) signals assumes negligible harmonic content in the recorded response. A broad frequency range over several decades will enable identification of the electrochemical and transport processes (e.g. double layer charging, charge transfer, interfacial capacitance, gas diffusion) taking place in the WE cell over a range of different time scales (i.e. 10^{-6} to 10^{3} s). The choice of the limits of the frequency range, and in particular its population, requires that the anticipated total measurement time is accounted for in order not to compromise the stability of the data measured when the cell is operated.

Particularly in PEMWE cells, EIS is principally used to optimise the structure of membrane electrode assemblies (MEAs) and to quantify changes in the parameters of the elements representative of the cell components in an electrical equivalent circuit (EEC) model to simulate cell impedance. Analysis by fitting EEC models to the impedance data obtained under different operating conditions facilitates determination of the contributions of the different physicochemical processes to the overall WE cell impedance in different conditions.

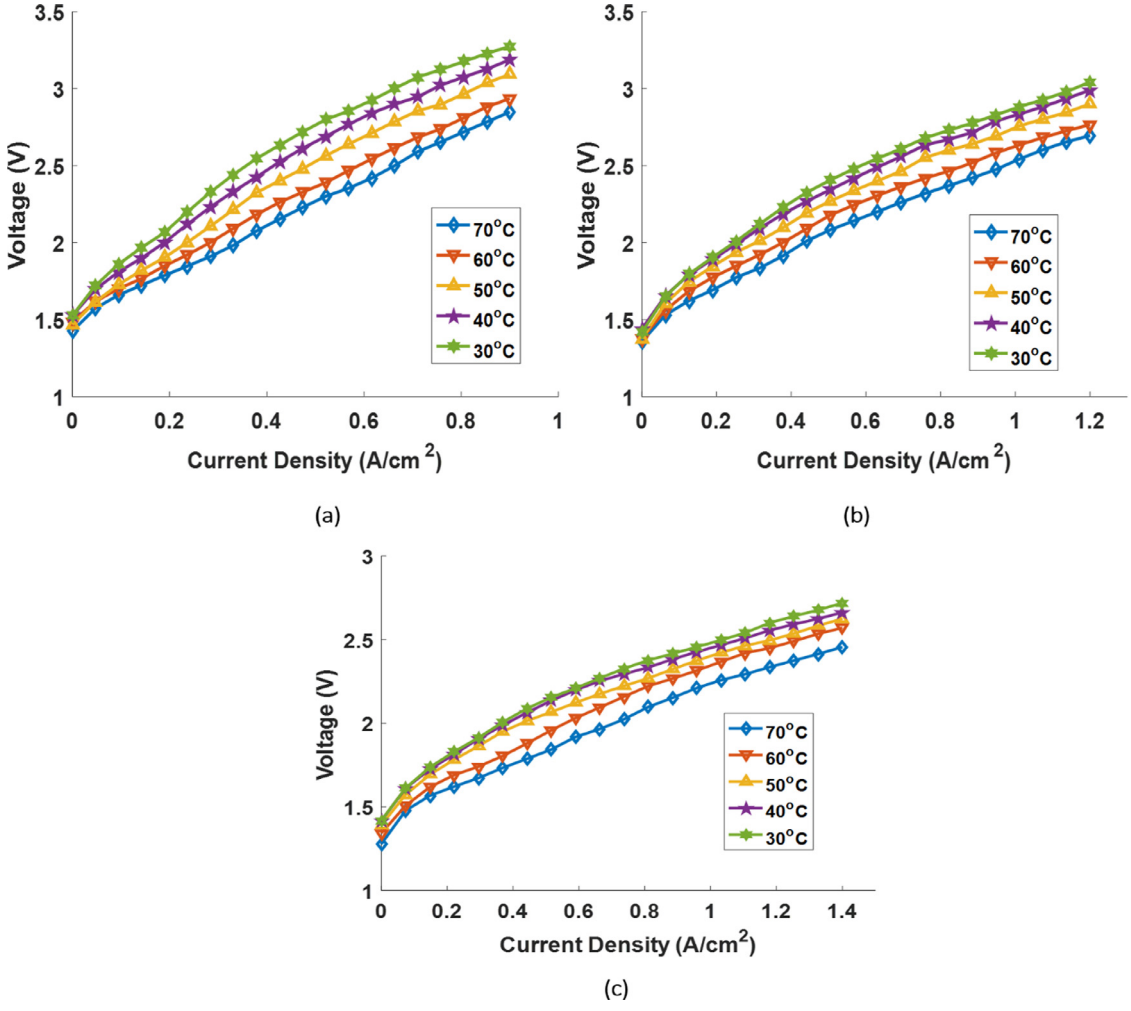

Fig. 12. Effect of temperature on the performance of PEM electrolyser with (a) Serpentine Flow Channel (b) Mesh Flow Channel and (c) OPCF Flow Channel.

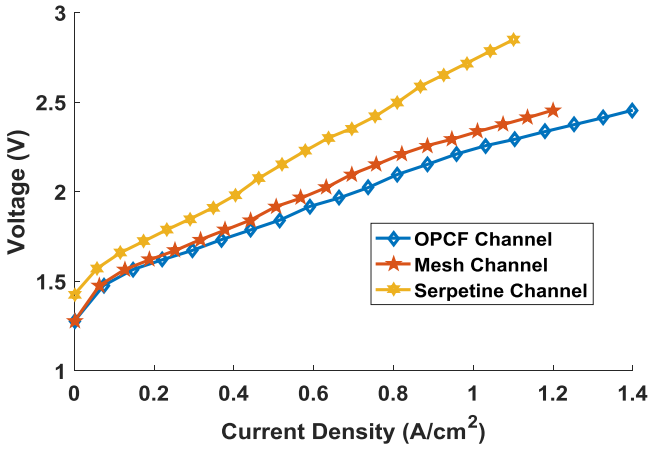

Fig. 13. Performance comparison for the three different types of flow channels operating at a constant temperature of 70°.

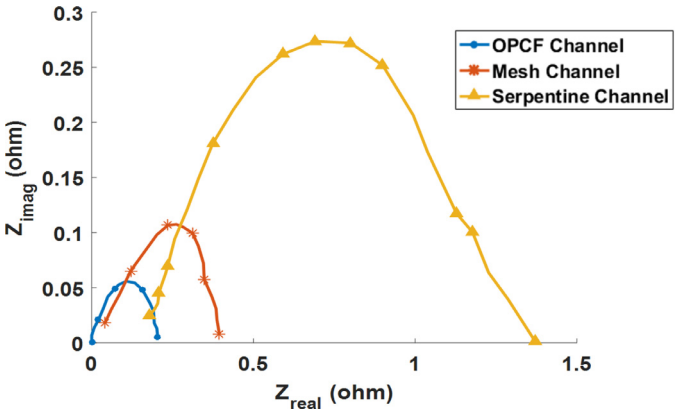

Fig. 14. EIS spectroscopy represented by a Nyquist plot for a PEM Electrolyser with different types of flow channels.

The main contributions to losses in WE performance (cell-voltage losses) are due to:

- ohmic resistance, associated with proton and electron conduction in the MEA, current collector and flow plates and
- electrode kinetics at the electrode/electrolyte interfaces and mass transport of reactant gases resulting collectively in the polarisation resistance.

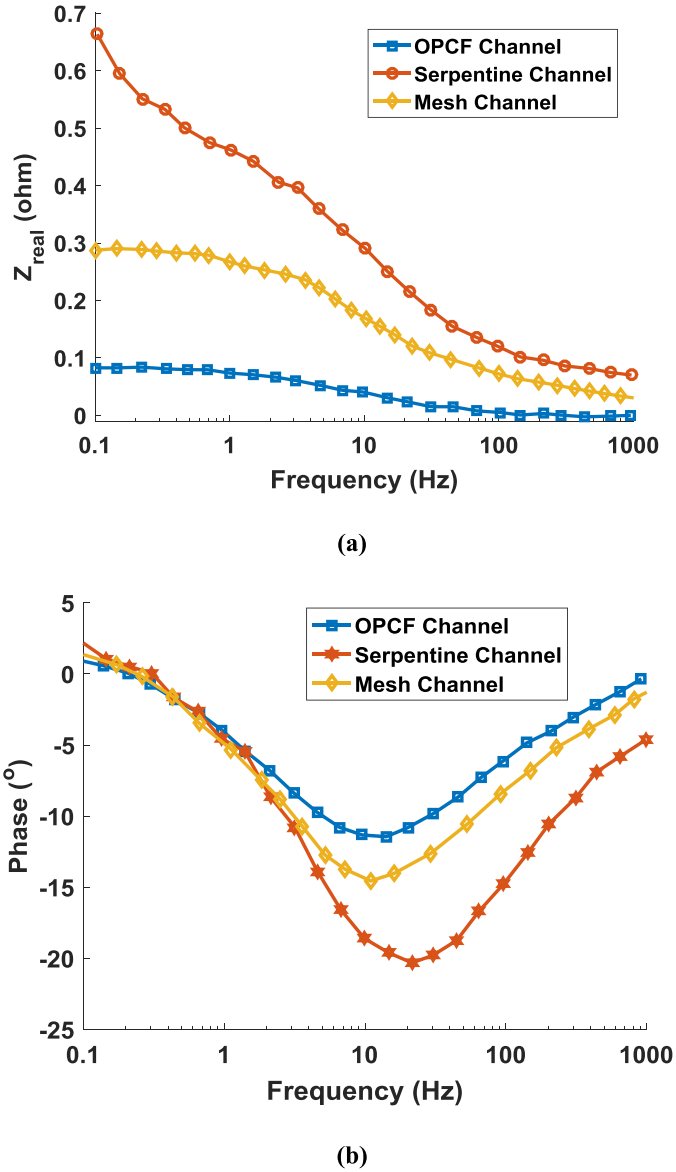

Fig. 15. Bode plot for PEM electrolyser with serpentine, mesh and OPCF channel (a) Frequency vs Impedance (b) Frequency vs Phase.

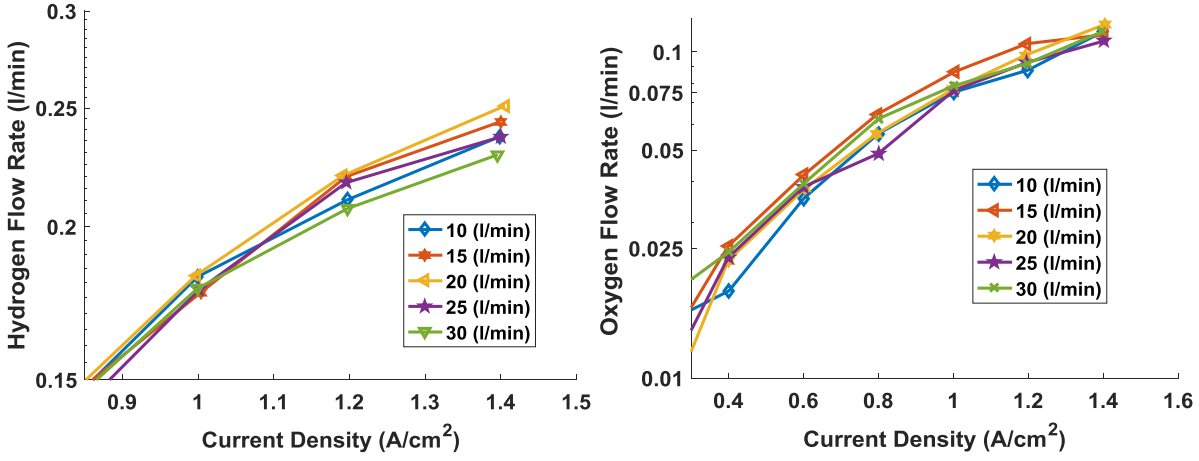

Fig. 16. Effect of varying water flow rates on both the hydrogen and oxygen flow rates for OPCF flow channel.

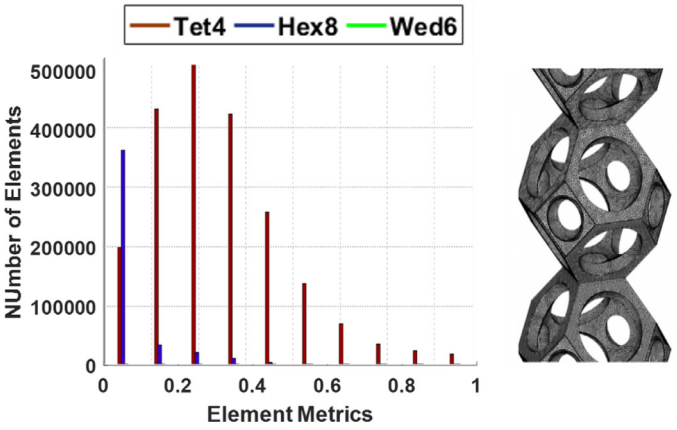

Fig. 17. Mesh Quality – Skewness factor check for OPCF material flow channel.

The reaction kinetics could be improved by using advanced catalysts and forming appropriate catalyst/electrolyte interfaces. Ohmic losses could be reduced by decreasing the hindrance on proton and electron movements within the membrane electrolyte, electrodes, monopolar/flow field plates, current collectors and their respective interfaces.

Therefore, EIS measurements in WE cell performance characterisation studies aim to:

- Identify individual contributions to the total WE cell impedance.
- Estimate other electrochemical parameters (double layer capacitance, charge transfer resistance, adsorption resistance, adsorption inductance, etc.) by complex non-linear least square (CNLS) analysis of an appropriate EEC model to simulate the measured impedance of the WE cell test set-up.
- Provide information that could assist in optimising WE cell components and operating conditions.

Other than the established fact that the increase in the performance of the PEM electrolyser is due to the lower pressure drop for the OPCF channel, electrochemical impedance spectroscopy was also performed on the three types of PEM electrolysers. An evident nature of electrical system is the fact that lower the resistance, the lower the losses within the system. The nature of the results shown in Fig. 14, clearly justifies the polarisation curve in Fig. 13, as the electrolyser with OPCF channel has a very low impedance than that of the serpentine channel and mesh channel. This low resistance is attributed to the losses within the PEMWE, i.e. the activation, ohmic and concentration losses. Also due to the uniform distribution of the species and water management, the water uptake within the membrane is significantly better for the OPCF channel electrolyser. As a result, the ionic conductivity of the membrane is higher than the serpentine and mesh channel electrolyser.

Fig. 15 shows the bode plots of the real impedance and the respective phase for serpentine, mesh and OPCF channel-based PEM electrolyser cells. The double layer capacitance in an electrolyser is a characteristic of any interface between an electron-conducting phase and an ion-conducting phase. It arises from the fact that (in the absence of a Faradaic process) charge cannot cross the interface when the potential across it is changed. The key component for the electrolyser dynamic behaviour is the capacitance of the cell. In Fig. 15(b) the phase angle equal to '0′ represent a pure ohmic resistance. For the frequency range between 5 Hz to 100 Hz the effect of impedance from charge transfer and electric double layer capacity can be seen. Above 100 Hz the effect of mass transfer can be seen. It is evident from the measured results that even at low frequencies the impedance of the electrolyser with OPCF channel is very small than the mesh and serpentine channel electrolyser cell as indicated by the frequency response in Fig. 15(a) and (b). This is due to the low resistance and high capacitance of the OPCF channel that provides homogenous flow of reactants to the membrane. At low frequencies the phase change is almost similar however at higher frequencies there is a deviation in the phases, where a higher phase deviation is observed for serpentine channel electrolyser than the OPCF channel electrolyser.

Further analysis on the effect of water flow rate was carried out to identify its effect on the OPCF channel electrolyser. Since the current density is highest at a water temperature of 70 °C, it is evident that the generating flow rates of hydrogen and oxygen will be high. Therefore, these values were measured in the typical water flow rate range from 10 to 30 ml/min in intervals of 5 ml/min as shown in Fig. 16 Because the PEM electrolyser generates hydrogen and oxygen with de-ionized water, the flow rates of hydrogen and oxygen increased as the input current density increased.

It is however indicative from the graphs that higher circulating water flow rates does not help in increasing the hydrogen or oxygen flow rates. From the generated results the highest hydrogen flow rate is observed at a water flow rate of 20 l/min and any flow higher than that causes a reduction in the generated hydrogen or oxygen flow rate. This is due to the residence time of the circulating water in the MEA where the conversion occurs. Also, this can be linked to the electrolyser entering a turbulent mode of operation where the higher flows are hindering its overall performance.

Table 1
Simulation Parameters used in ANSYS Fuel Cell & Electrolyser Module.

Anode		Cathode	
Reference Current Density (A/m^2)	10,000	Reference Current Density (A/m^2)	20
Reference Concentration ($kmol/m^3$)	1	Reference Concentration ($kmol/m^3$)	1
Concentration Exponent	0.5	Concentration Exponent	1
Exchange Coefficient (a)	2	Exchange Coefficient (a)	2
Exchange coefficient (c)	2	Exchange coefficient (c)	2
Reference Diffusivity			
H2 (m2/s)		3×10^{-5}	
O_2 (m^2/s)		3×10^{-5}	
H_2O (m^2/s)		3×10^{-5}	
Other Species		3×10^{-5}	

Table 2
Boundary conditions.

Interface	Type	Value	Thermal	Species		
				H_2	O_2	H_2O
Anode Inlet	Velocity Inlet	1	343K	0	0	1
Anode Outlet	Pressure Outlet	0	343K	0	0	0
Cathode Inlet	Velocity Inlet	0	343K	0	0	0
Cathode Outlet	Pressure Outlet	0	343K	0	0	0
Anode Current Collector	Wall	1.3 V – 1.8V	343K	N/A		
Cathode Current Collector	Wall	0	343K	N/A		

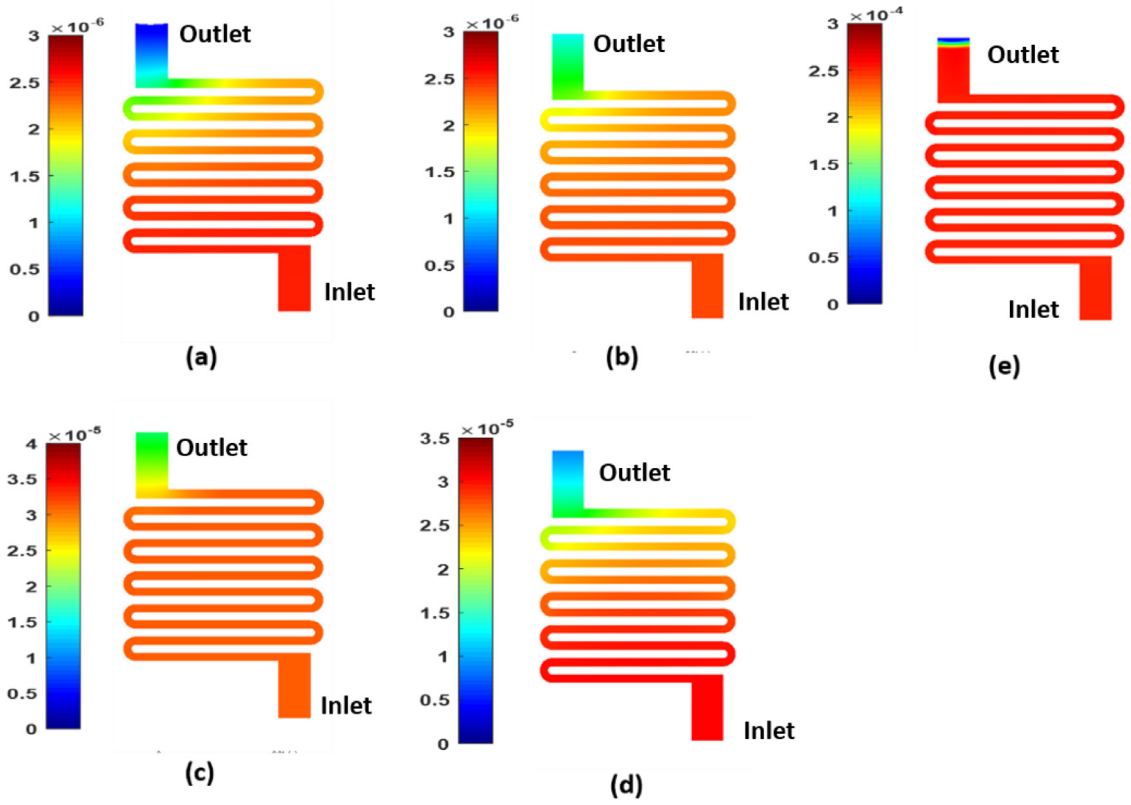

Fig. 18. Concentration (kmol/m^3) of hydrogen at the serpentine cathode channel for simulated voltage levels (a) 1.3 V (b) 1.4 V (c) 1.5 V (d) 1.6 V (e) 1.7 V.

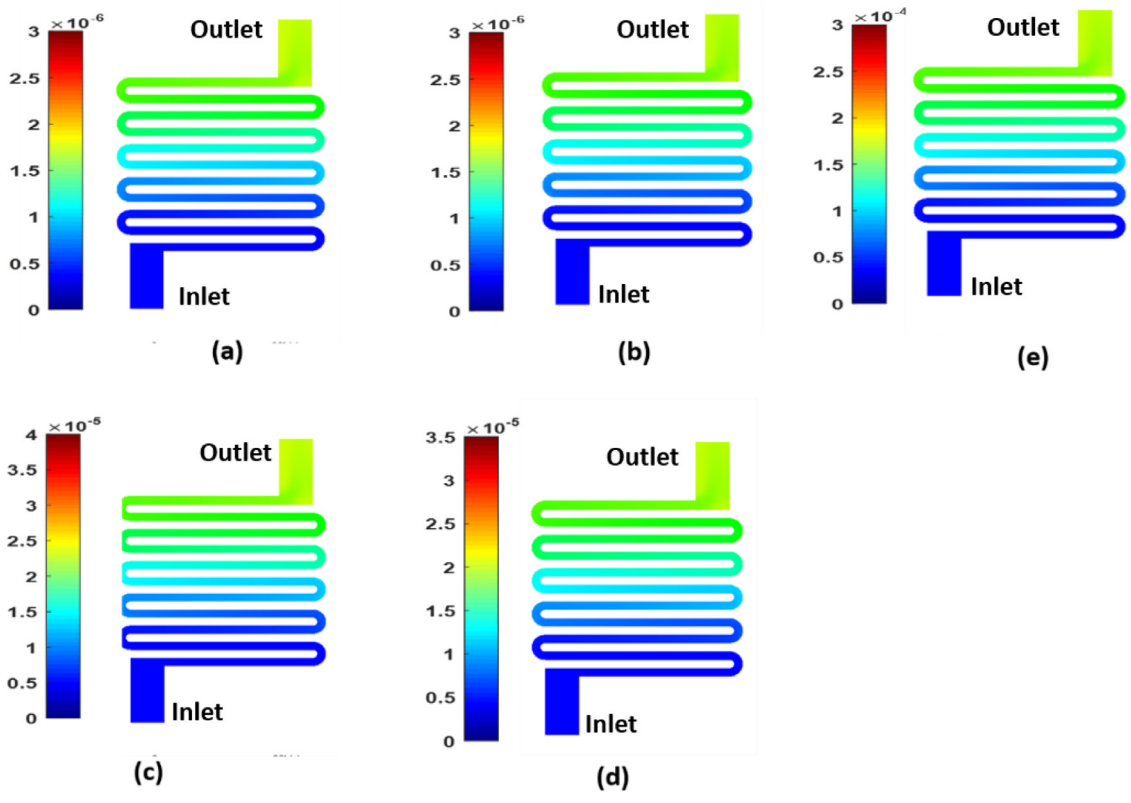

Fig. 19. Concentration (kmol/m^3) of oxygen at the serpentine anode channel for simulated voltage levels (a) 1.3 V (b) 1.4 V (c) 1.5 V (d) 1.6 V (e) 1.7 V.

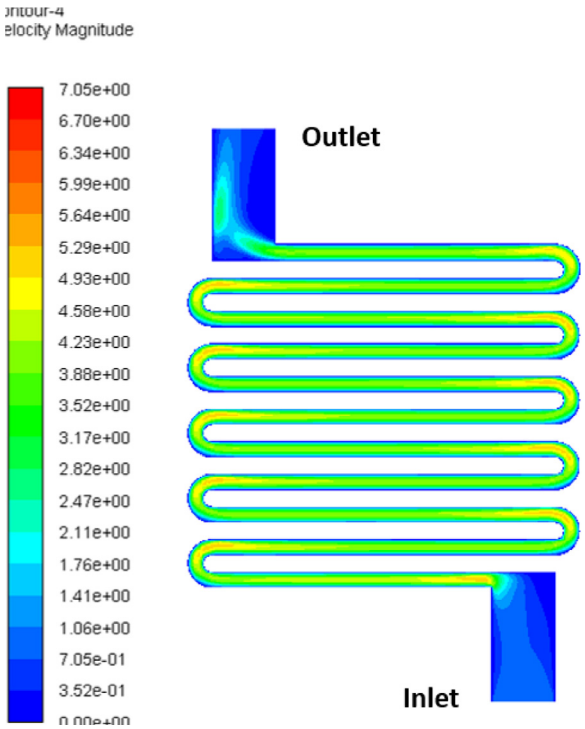

Fig. 20. Even distribution of the velocity field in the anode stream.

4.2. Numerical results and discussions

Computational Fluid Dynamic (CFD) modelling tools and many researchers employed CFD tools in their studies to develop and optimize the bipolar flow plates. ANSYS, Inc. is an engineering simulation software (computer aided engineering or CAE) developer that makes use of CFD, FEM and some various types of programming algorithms for simulation and optimization. Any project simulation conducted in ANSYS involves five steps for the completion of the project (geometry creation, meshing, simulation setup, running the calculations and post processing). CFD programs are often used to predict the flow patterns and regimes, velocity profiles, and pressure gradients in parts of the fuel cell components or through the full flow plates and flow fields. The flow plates used in this study are designed to cover an active area of approximately 115 cm^2. This is basically the active area being used by the electrolyser MEA. Some of the key parameters which are very necessary to consider when designing a flow plate channel layout are the distribution of pressure on the GDL and membrane, pressure drop in and through the flow plate, distribution of temperature on the GDL and membrane, consistent reactant concentration over the whole active area of the GDL and membrane, membrane hydration and mitigation of flooding. To validate the numerical model it must be in perfect agreement with the results from the experiment conducted. From the results gathered for both scenarios, they were in perfect agreement, showing the validity of the numerical model which can be seen in the later part of Section 4.2.1.

4.2.1. Mesh quality and dependence

One of the key steps in the CFD simulation process is the creation of the mesh. The collection of differential and algebraic equations that describe the process are solved (approximated) using different techniques at these mesh elements. The meshing process breaks the domain in small entities that constitute the mesh. For a valid CFD simulation, the results obtained need to be independent of the mesh size or the type of elements used, and convergence studies are

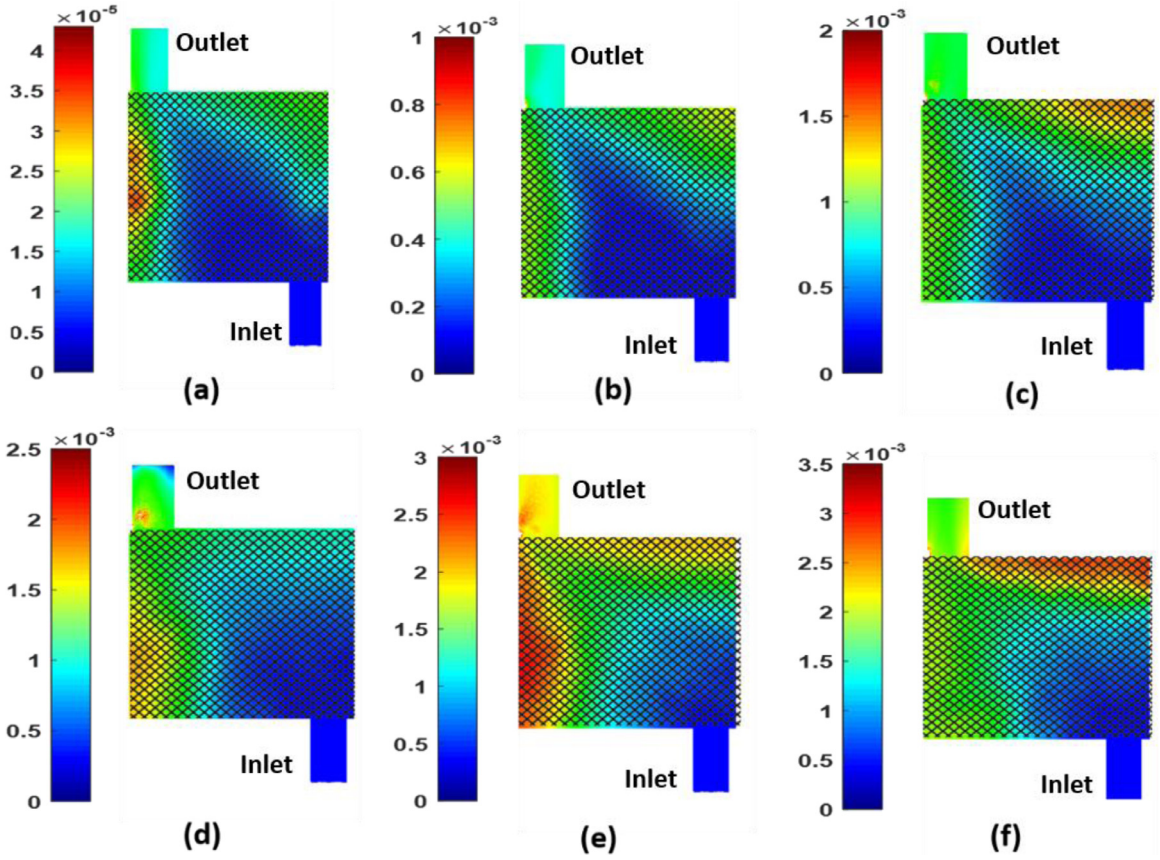

Fig. 21. Concentration (kmol/m^3) of hydrogen at the mesh cathode channel for simulated voltage levels (a) 1.3 V (b) 1.4 V (c) 1.5 V (d) 1.6 V (e) 1.7 V (f) 1.8 V.

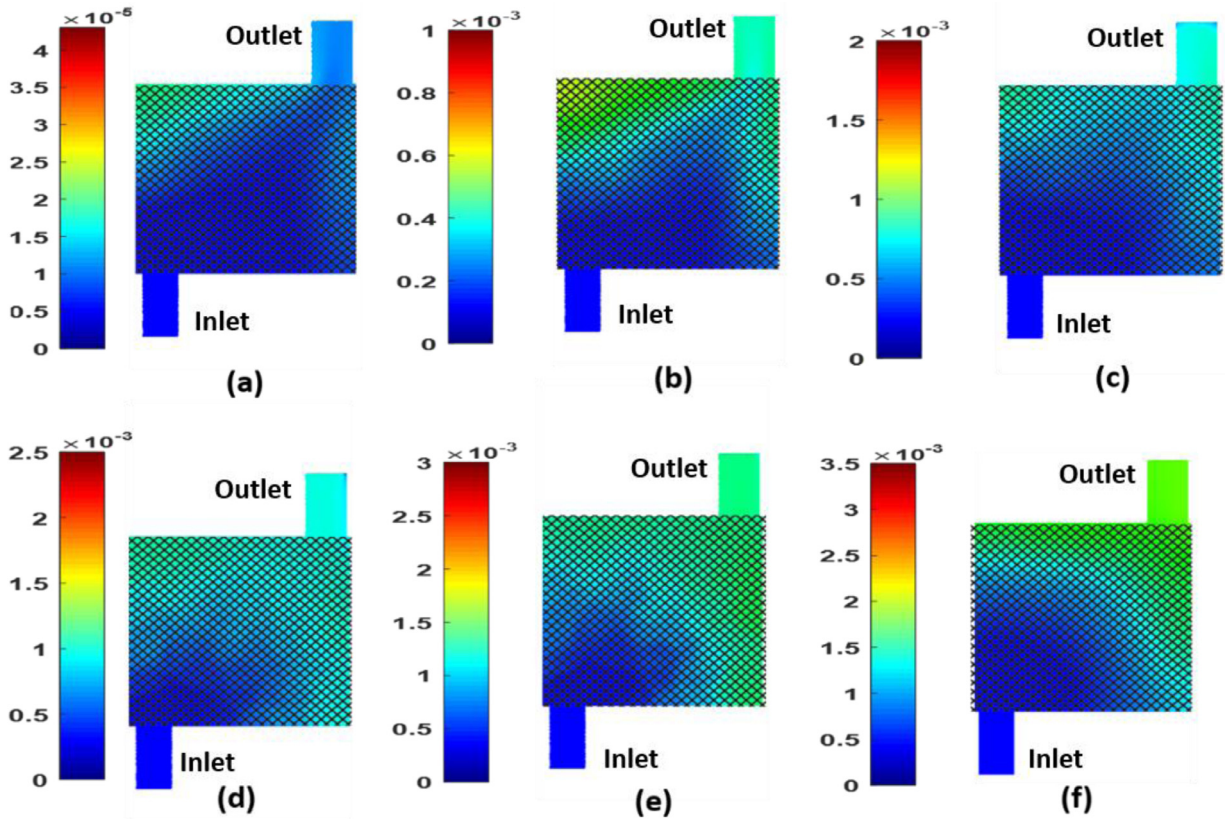

Fig. 22. Concentration (kmol/m^3) of Oxygen at the mesh anode channel for simulated voltage levels (a) 1.3 V (b) 1.4 V (c) 1.5 V (d) 1.6 V (e) 1.7 V (f) 1.8 V.

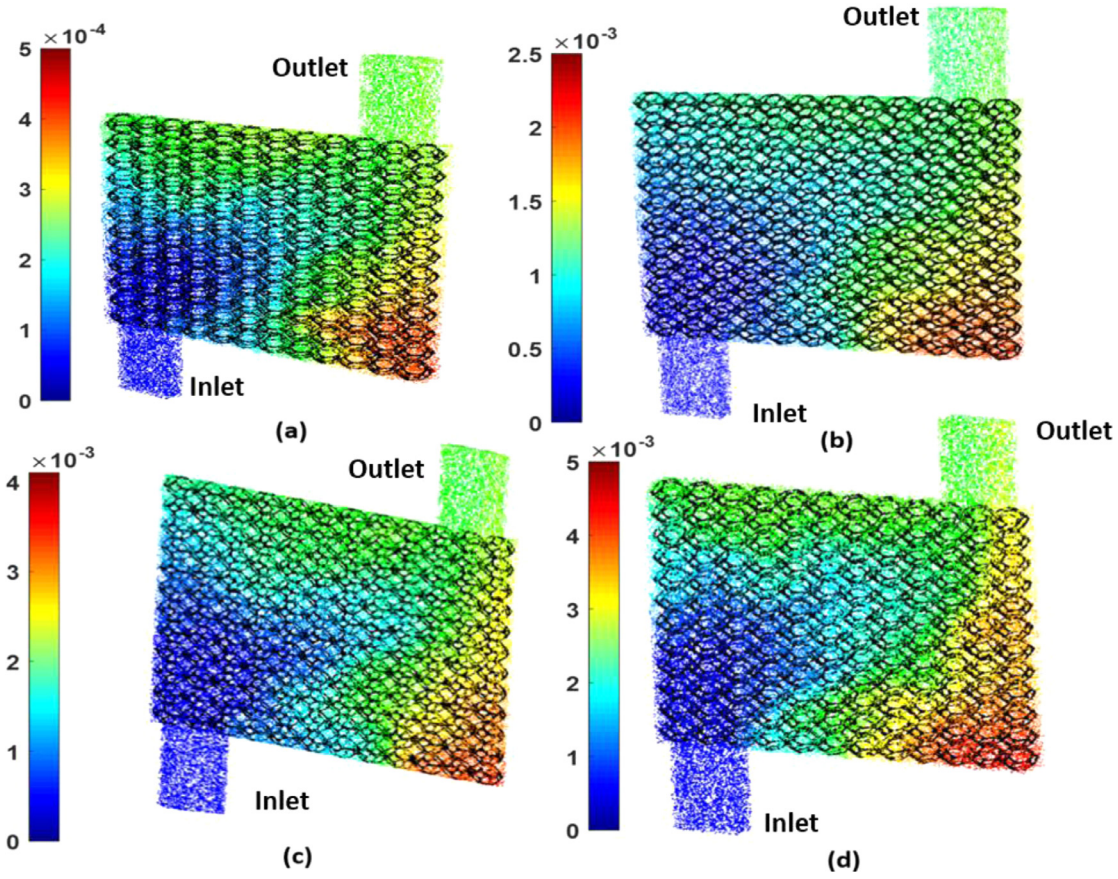

Fig. 23. Concentration of Hydrogen (kmol/m^3) at the OPCF cathode channel for simulated voltage levels (a) 1.3 V (b) 1.5 V (c) 1.7 V (d) 1.8 V.

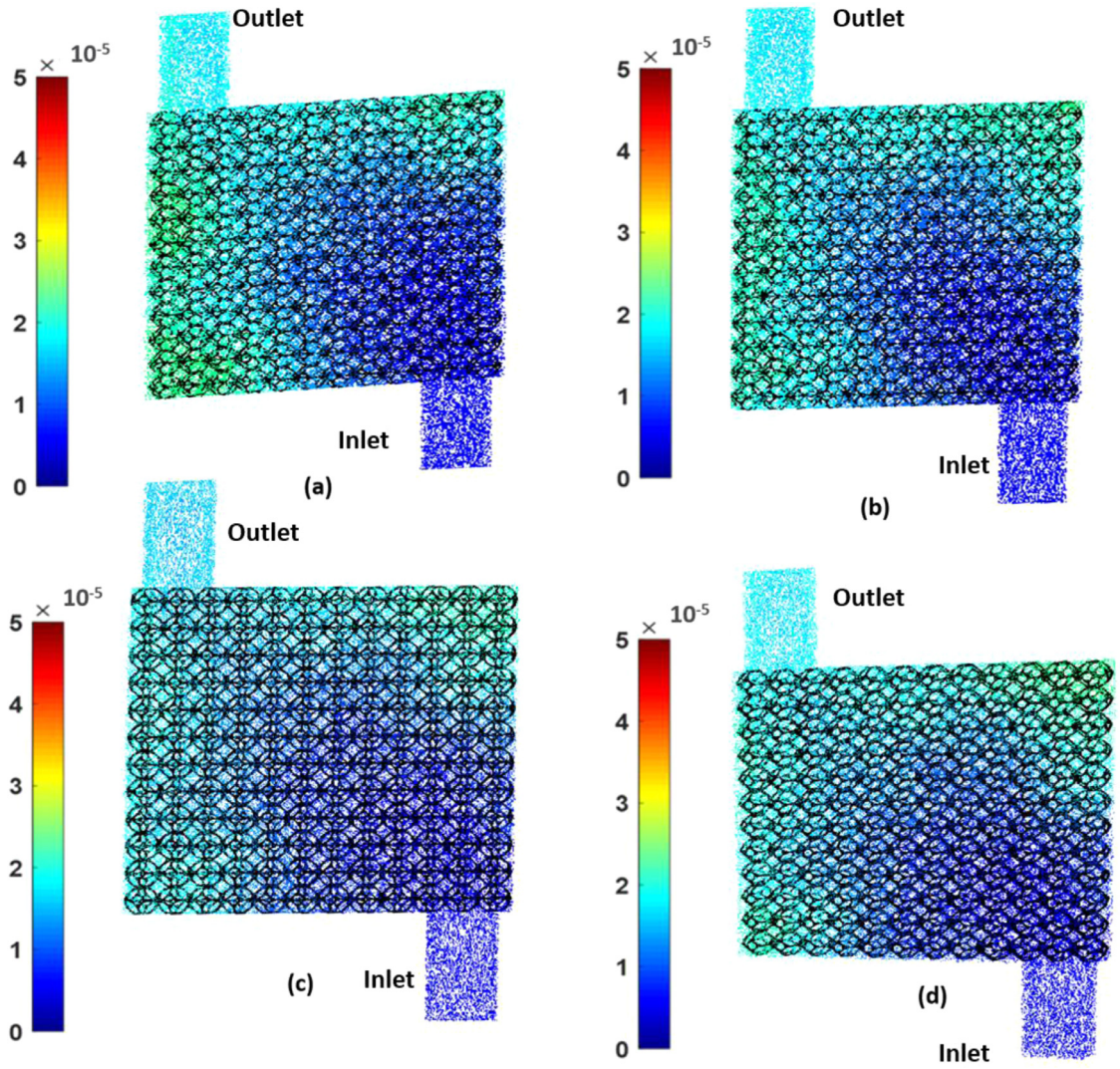

Fig. 24. Concentration of Oxygen (kmol/m^3) at the OPCF anode channel for simulated voltage levels (a) 1.3 V (b) 1.5 V (c) 1.7 V (d) 1.8 V.

necessary to ensure this. The size of the mesh and grid elements types can be modified by using the controls of the meshing engine of ANSYS.

The quality of the mesh plays a significant role in the accuracy and stability of the numerical computation. The attributes associated with mesh quality are node point distribution, smoothness, and skewness. Regardless of the type of mesh used in a domain, checking the quality of mesh is essential. Depending on the cell types in the mesh (tetrahedral, hexahedral, polyhedral, etc.), different quality criteria are evaluated.

In this investigation, three different designs with complex geometries were studied. This therefore required an overall different mesh dependency test and a different element size for each of the flow plate assemblies. The most complex geometry studied is the open pore cellular foam material channel. One of the main aspects widely used in ANSYS simulation is the skewness, which has a significant impact on the accuracy of the numerical solution. ANSYS specifies that "a general rule is that the maximum skewness for a triangular/tetrahedral mesh in most flows should be kept below 0.95, with an average value that is less than 0.33. A maximum value above 0.95 may lead to convergence difficulties. Therefore, the mesh quality criteria for all the simulations carried out was set to a lower skewness as shown in Fig. 17. In the case of OPCF material flow channel, ANSYS uniform meshing was considered, with a maximum number of nodes of 1,100,523 and around 2,524,879 number of elements.

Once the mesh was carefully studied and validated, the rest of the modifications to be made on the existing flow plates were simulated in CFD with finely divided grid. This helps improves the resolution and gives better prediction of the pressure drop that occurs through the selected fluid domain. The next stage of the simulation process is to carry out simulations for the different flow channels used in the making of PEM electrolyser.

The serpentine flow channel design has been widely studied and implemented by several researchers around the world and it is considered as the standard for flow design in most fuel cells. Several companies use this design as their main flow plate design in manufacturing of PEM fuel cells because it supports the full usage of the active area and coverage of gas at reasonable pressure losses. In this work this design was used to draw a comparison on different flow channels. Table 1 shows the simulation parameters and the properties used. Table 2 shows the boundary conditions for the CFD analysis in ANSYS.

In order to evaluate the effect of flow channel on the performance of electrolyser, all the boundary conditions were kept similar in all the simulations. The mesh quality as discussed was set to skewness metrics and a total of 800 iterations were carried out to get

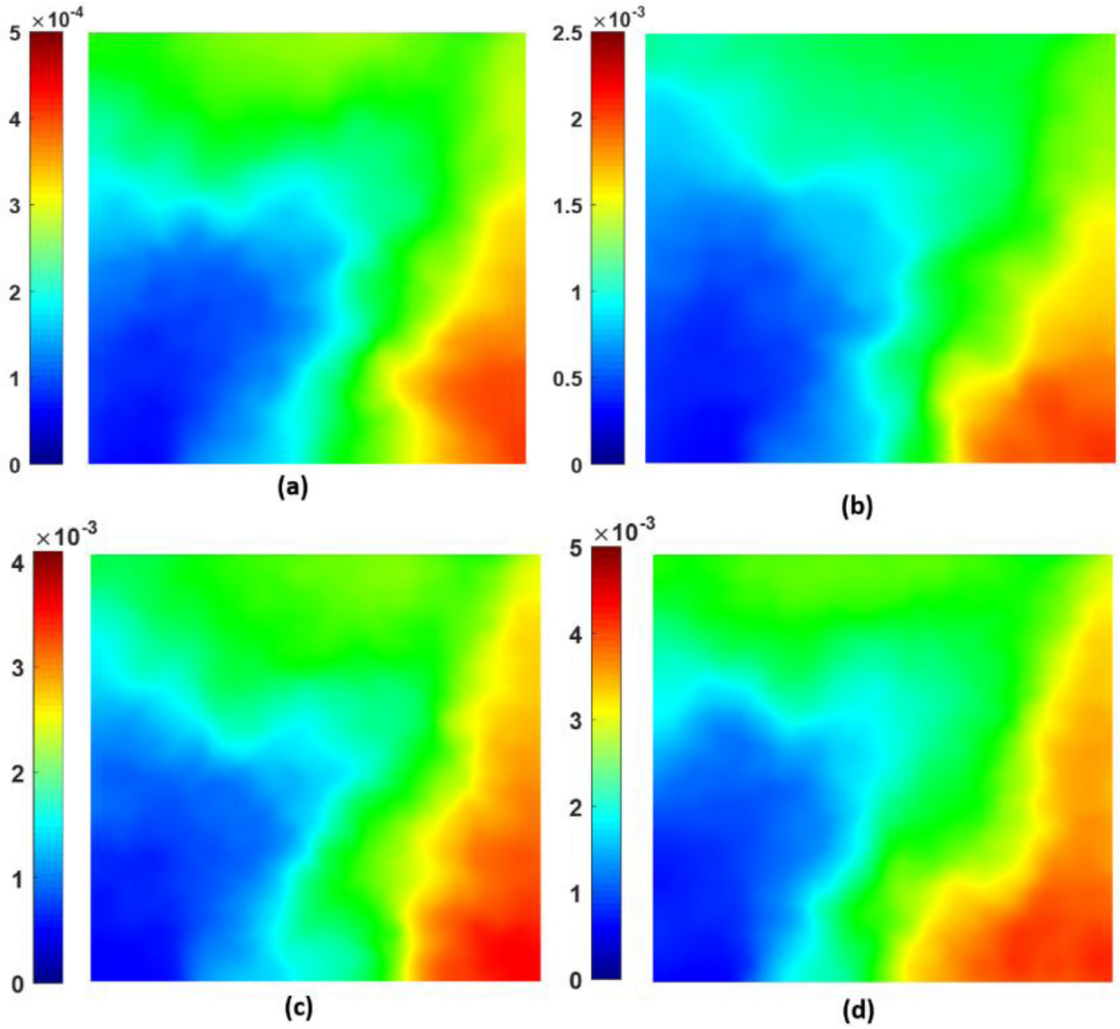

Fig. 25. Concentration of Hydrogen at the cathode interface of the membrane (kmol/m^3) for simulated voltage levels (a) 1.3 V (b) 1.5 V (c) 1.7 V (d) 1.8 V.

converging results. ANSYS simulation of the 'fuel cell and electrolyser module' takes into consideration of the energy balance between the anode and the cathode. This energy balance is based on several factors such as the types of species (H_2, O_2, H_2O), temperature, and the boundary conditions acting on it. By determining the voltage level at the current collector, the energy equation evaluates the corresponding current density required for the electrolyser to generate the species, laminar flow within the channels and membrane dynamics. In the simulation, the conversion criteria was set on the energy equation, with a tolerance of $1e^{-6}$.

Fig. 18 and Fig. 19 shows the concentration of hydrogen and oxygen in the serpentine flow channel of the PEM electrolyser at the cathode and anode respectively. Around 800 iterations were carried out to get convergence for each set of results beginning from 1.3 V to 1.7 V as shown in Fig. 18(a) – (e) and Fig. 19(a) – (e). Hydrogen and oxygen concentration increase with increasing voltage. Fig. 18(a) to 18(e) shows the effect of input voltage on the concentration of hydrogen in the serpentine channels. Since the temperature set at the boundary of the electrolyser was at 313 K (40 °C) there was not enough energy for the electrolyser to generate ample amount of hydrogen. This can be seen in Fig. 18(a) where the blue region in the outlet of the serpentine channel suggest no hydrogen leaving the channel. Most of the hydrogen that is generated is in the bottom half of the channel. On applying higher voltages, the amount of hydrogen being produced is higher and is based on the amount of current. The evolution of amount of hydrogen at the outlet can be seen to increase with the highest concentration at the outlet as shown in Fig. 18(e) at 2.8×10^{-2} kmol/m^3. It is a known fact that however serpentine channel provides a full MEA coverage for the reactant, due to the high-pressure losses the serpentine channel provides a lower overall performance. There is a high inlet pressure on the inlet channels. This pressure gradually drops from the inlet to the outlet, a clear indication that the pressure within the MEA decreases from inlet to the outlet as expected. The mass transport and the general performance of the electrolyser are governed by these characteristics of the PEM electrolyser. There is an even distribution of the velocity field of the water throughout the entire flow plate and the flow covers the full area of the MEA being supplied with the reactant (Deionised water) as shown in Fig. 20. The serpentine flow plate design ensures a constant flow of the fluid through the channels and this in effect helps remove any excess liquid that may condense in the electrolyser such as water that may block the channels by transporting it to the outlet easily. However, any gas that is generated will not be able to escape the channel due to the constant flow of the reactant. The results indicate that the use of serpentine channel for electrolyser will work but it is not efficient way of producing hydrogen.

Fig. 21 and Fig. 22 shows the concentrations of hydrogen and oxygen for a mesh channel PEM electrolyser. In comparison to the serpentine channel where the gas flow was only available through the serpentine channel only, the concentration at the very beginning of

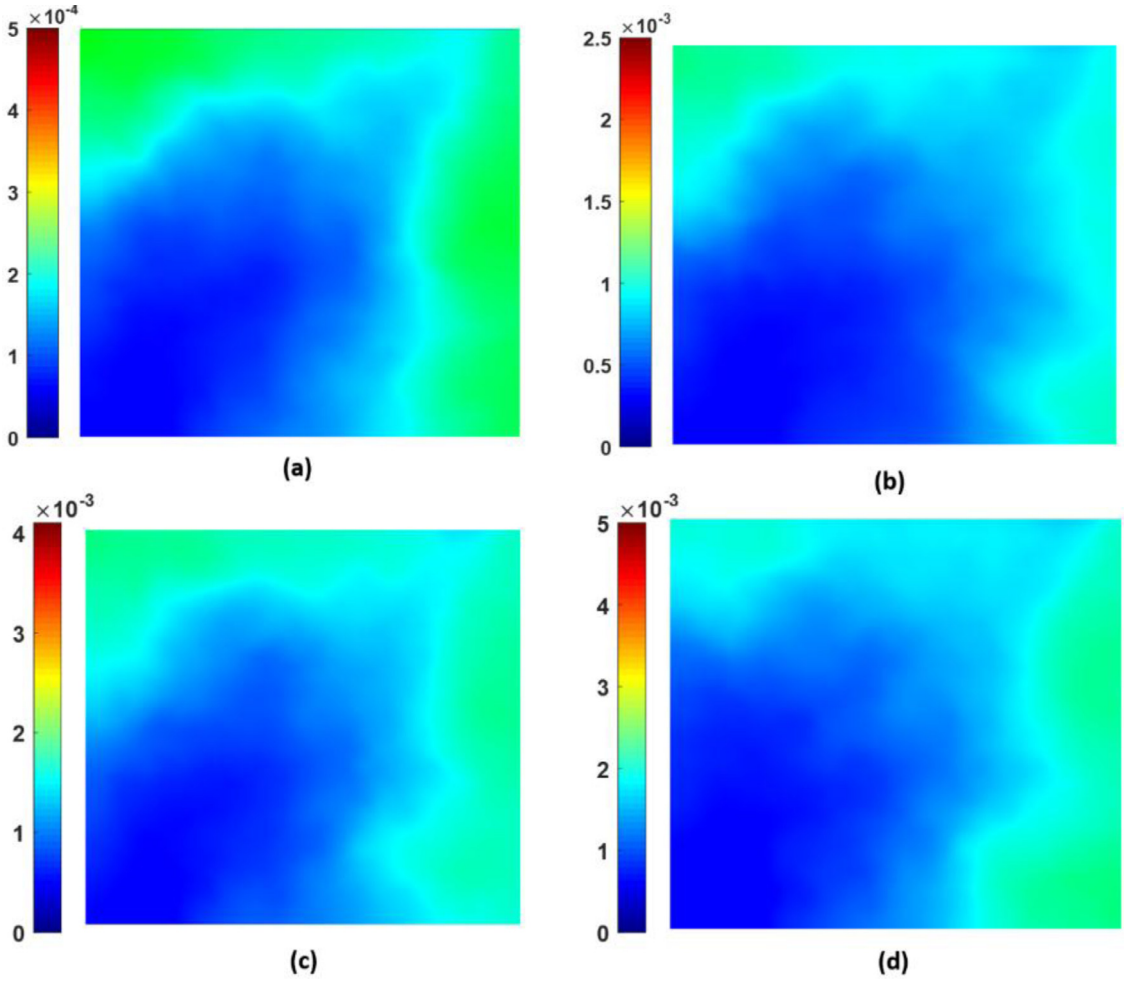

Fig. 26. Concentration of Oxygen at the anode interface of the membrane (kmol/m^3) for simulated voltage levels (a) 1.3 V (b) 1.5 V (c) 1.7 V (d) 1.8 V.

was very low at the outlet of the channel. However, the mesh channel shows a clear indication that due the geometry of the flow channel the generated hydrogen and oxygen has an easier passage to escape. This can be seen by the green colour clearly indicating significant amount of hydrogen is escaping at the outlet as shown in Fig. 21(a) – (f). Also as the voltage begins to increase, the amount of current also increases. This increase is indicative of the increase in the hydrogen and oxygen concentration in both Fig. 21 and Fig. 22. A ten times higher concentration of hydrogen gas of 1.5×10^{-3} kmol/m^3 is recorded for Mesh flow channel at 1.7 V to that observed for the serpentine flow channel of 1.5×10^{-4} kmol/m^3 at the same voltage level.

Fig. 23 shows the concentration of hydrogen in the cathode channels. These are indicated by the path lines. The path lines shows the flow of the gas through and upward at the outlet of the channel. A significant difference is seen in the performance of the electrolyser as indicated by the concentration levels at the outlet. Due to the increase in the pore size provided by the foam and a uniform geometric flow of the reactant, which covers the entire region of the membrane – it provides an overall increase in the performance of the electrolyser. This can be seen in comparison to Fig. 23 where the OPCF channel at 1.7 V provides a concentration at the outlet of 2.2×10^{-3} kmol/m^3 which is 1.5 times higher than that of the mesh channel observed at the same voltage level.

Fig. 24

Fig. 25 and Fig. 26 show the concentration of the hydrogen and oxygen at the respective membrane interface to the cathode and anode part of the channel. The distribution of hydrogen and oxygen concentration provide a definitive indication that the hydrogen and oxygen gases are escaping the channel more efficiently than that observed for either serpentine or mesh flow channels.

Fig. 27 draws a comparison on the performance of the electrolyser using different flow plates. These results have been evaluated by taking the steady state value of hydrogen and oxygen concentration at the outlet of the flow plates. The measured value is after successful convergence of the data. It can be seen from Fig. 27(a) and (b) that both hydrogen and oxygen concentration increase significantly using the OPCF channel in comparison to the other flow plates.

Fig 28 shows the polarisation curve for the simulation results obtained after individual iterations for each type of electrolyser with different flow channels. During the simulation it was observed that for the case of serpentine channel, the results never converged beyond a cell voltage of 1.7 V. However for the case of mesh and OPCF flow channels the results converged beyond 1.8 V. The polarisation curve clearly distinguishes the performance of the electrolyser based on the type of flow channel used. It can be seen that the performance of the OPCF flow channel electrolyser is 1.5 times higher than that of the mesh channel electrolyser where a current density of 1.2A/cm^2 is recorded for OPCF channel electrolyser.

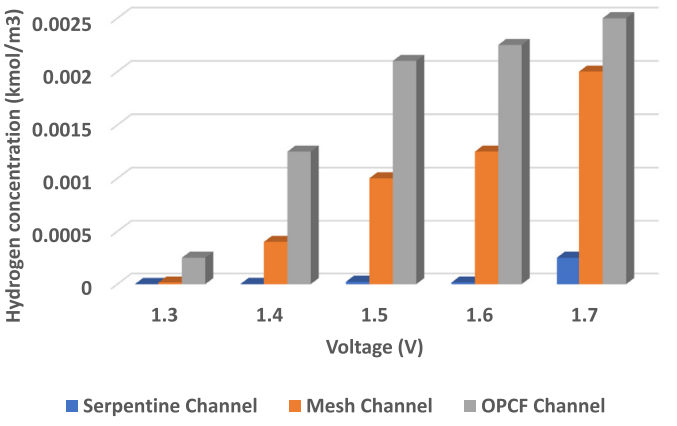

(a)

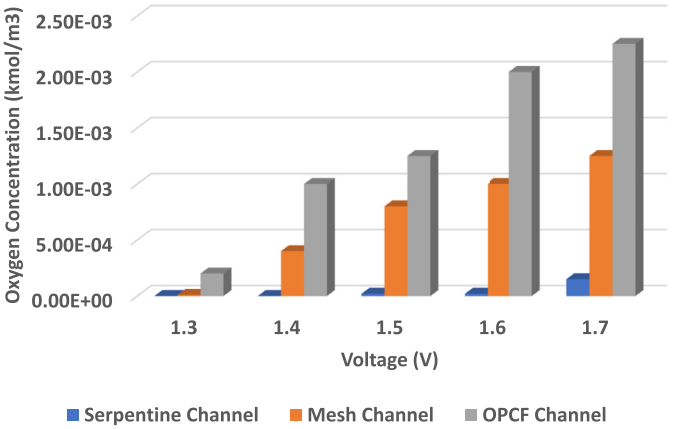

(b)

Fig. 27. Concentration of (a) hydrogen and (b) oxygen for different flow plate channels. The results indicate peak concentration at the outlet of the flow plate at voltages 1.3 V to 1.7 V.

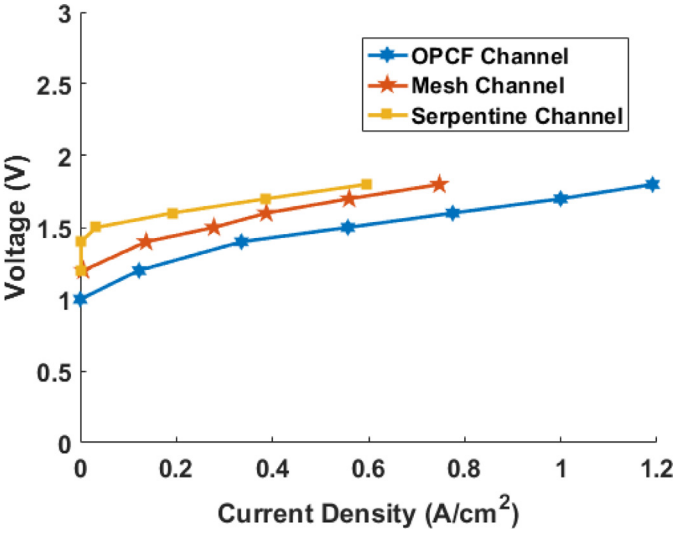

Fig. 28. Polarisation curves for serpentine, mesh and OPCF channel PEM electrolyser.

Conclusion

The general performance of an electrolyser depends highly on the pressure drop as well as the velocity of the water as it flows through the flow channel. High drop in pressure indicates that the flow of water to the reactive site would be low. Therefore, the rate at which hydrogen will be released due to the electrochemical reaction will be lower. To increase the overall performance of the electrolyser different types of flow channels were considered. Initial investigation was carried out using PEM fuel cells, as open pore cellular foam material flow channels have been widely studied and have shown better overall performance.

In order to analyse the effect of OPCF material on the performance of PEM electrolysers, 3D CFD simulations were carried out in ANSYS Fluent using the fuel cell and electrolyser module available in that package. It was found that in within the voltage range of 1.3 – 1.7 V, the OPCF material flow channel had the highest oxygen and hydrogen concentration. Compared to the performance at 1.3 V the concentrations increased 10 times at 1.7 Vs for the OPCF channel achieving a steady state hydrogen concentration of 2.5×10^{-3} kmol/m^3 .

A study on the effect of the type of flow channel was also undertaken by performing a series of laboratory experiments. A balance of plant was created for the electrolyser. Water flow rate and temperature of the water was varied to assess the effect on the performance of the electrolyser based on three different types of flow channels. It was found that the OPCF material flow channel operating at a temperature of 70 °C and water flow rate of 20 l/min gave the best performance amongst other electrolyser assemblies. The experimental results show that using an OPCF flow plate (porous channel) outperformed the mesh and serpentine flow plate, recording 2.5 V at 1.4A/cm^2. This is in excess of approximately 17% improvement on the current density of the benchmark mesh flow plate under the same operating conditions operating at 2.5 V.

Ohmic losses are one of the key performance metrics and high resistances are indicative of low performing electrolysers. Electrochemical impedance spectroscopy was therefore performed at open circuit voltage conditions and it was found by the Nyquist plot that OPCF material flow channel provided the lowest resistance compared with other flow plates. A vey small resistance of 0.3 ohm was measured in comparison to 1.2 ohm for the serpentine channel electrolyser. The work finally concluded that, in comparison to the serpentine and mesh flow design, the open pore cellular foam material was a suitable option for a PEM electrolyser.

Declaration of Competing Interest

None.

References

1. Hussam Jouhara, Alina Żabnieńska-Góra, Navid Khordehgah, DaremA hmad, Tom Lipinski, Latent thermal energy storage technologies and applications: a review, Int. J. Thermofluids 5–6 (August 2020) 100039 Volumes, doi: 10.1016/j.ijft.2020.100039.
2. Tabbi Wilberforce, Ahmad Baroutaji, Bassel Soudan, Abdul Hai Al-Alami, Abdul Ghani Olabi, Outlook of carbon capture technology and challenges, Sci. Total Environ. Vol. 657 (20 March 2019) 56–72, doi: 10.1016/j.scitotenv.2018.11.424.
3. Tabbi Wilberforce, A. Baroutaji, Zaki El Hassan, J. Thompson, Bassel Soudan, A.G. Olabi, Prospects and challenges of concentrated solar photovoltaics and enhanced geothermal energy technologies, Sci. Total Environ. 659 (1 April 2019) 851–861, doi: 10.1016/j.scitotenv.2018.12.257.
4. Tabbi Wilberforce, Zaki El Hassan, A. Durrant, J. Thompson, Bassel Soudan, A.G. Olabi, Overview of ocean power technology, Energy Vol. 175 (15 May 2019) 165–181, doi: 10.1016/j.energy.2019.03.068.
5. Hussam Jouhara, Nicolas Serey, Navid Khordehgah, Robert Bennett, Sulaiman Almahmoud, Stephen P.Lester, Investigation, development and experimental analyses of a heat pipe based battery thermal management system, Int. J. Thermofluids 1–2 (February 2020) 100004 Volumes.
6. T. Wilberforce, F.N. Khatib, E. Ogungbemi, A.G. Olabi, Water electrolysis technology, Ref. Modul. Mater. Sci. Mater. Eng., Elsevier (2018), doi: 10.1016/B978-0-12-803581-8.11273-1.
7. Ahmad Baroutaji, Tabbi Wilberforce, Mohamad Ramadan Abdul Ghani Olabi, Comprehensive investigation on hydrogen and fuel cell technology in the aviation and aerospace sectors, Renew. Sustain. Energy Rev. 106 (May 2019) 31–40, doi: 10.1016/j.rser.2019.02.022.
8. G.G. Scherer, T. Momose, K. Tomiie, Membrane water electrolysis cells with a fluorinated cation exchange membranes, J. Electrochem. Soc. 145 (1988) 780.

9. T. Wilberforce, Z. El-Hassan, F.N. Khatib, A. Al Makky, J. Mooney, A. Barouaji, et al., Development of Bi-polar plate design of PEM fuel cell using CFD techniques, Int. J. Hydrog. Energy (2017), doi: 10.1016/j.ijhydene.2017.08.093.
10. O.S. Ijaodola, Zaki El- Hassan, E. Ogungbemi, F.N. Khatib, Tabbi Wilberforce, James Thompson, A.G. Olabi, Energy efficiency improvements by investigating the water flooding management on proton exchange membrane fuel cell (PEMFC), Energy 179 (15 July 2019) 246–267.
11. S. Song, H. Zhang, X. Ma, Z. Shao, R.T. Baker, B. Yi, Electrochemical investigation of electrocatalysts for the oxygen evolution reaction in PEM water electrolyzers, Int. J. Hydrog. Energy 33 (2008) 4955–4961.
12. J.L. Weininger, R.R. Russell, Corrosion of ruthenium oxide catalyst at anode of a solid polymer electrolyte cell, J. Electrochem. Soc. 125 (9) (1978) 1482–1486.
13. F. Andolfatto, R. Durand, A. Michas, P. Millet, P. Stevens, Solid polymer electrolyte water electrolysis - electrocatalysis and long-term stability, Int. J. Hydrog. Energy 19 (5) (1994) 421–427.
14. X. Wu, J. Tayal, S. Basu, K. Scott, Nano-crystalline $RuxSn_{1-}xO_2$ powder catalysts for oxygen evolution reaction in proton exchange membrane water electrolysers, Int. J. Hydrog. Energy 36 (22) (2011) 14796–14804.
15. K. Kadakia, M.K. Datta, O.I. Velikokhatnyi, P. Jampani, S.K. Park, P. Saha, et al., Novel $(Ir,Sn,Nb)O_2$ anode electrocatalysts with reduced noble metal content for PEM based water electrolysis, Int. J. Hydrog. Energy 37 (4) (2012) 3001–3013.
16. M. Budt, D. Wolf, R. Span, J. Yan, A review on compressed air energy storage: basic principles, past milestones and recent developments, Appl Energy 170 (2016) 250–268.
17. Tabbi Wilberforce, O. Ijaodola, Emmanuel Ogungbemi, F.N. Khatib, T. Leslie, Zaki El-Hassan, J. Thomposon, A.G. Olabib, Technical evaluation of proton exchange membrane (PEM) fuel cell performance – a review of the effects of bipolar plates coating, Renew. Sustain. Energy Rev. 113 (October 2019) 109286, doi: 10.1016/j.rser.2019.109286.
18. U. Desideri, F. Zepparelli, V. Morettini, E. Garroni, Comparative analysis of concentrating solar power and photovoltaic technologies: technical and environmental evaluations, Appl. Energy 102 (2013) 765–784.
19. F.N. Khatib, Tabbi Wilberforce, Oluwatosin Ijaodola, Emmanuel Ogungbemi, Zaki El-Hassana, A. Durrant, J. Thompson, A.G. Olabi, Material degradation of components in polymer electrolyte membrane (PEM) electrolytic cell and mitigation mechanisms: a review, Renew. Sustain. Energy Rev. (111) (September 2019) 1–14, doi: 10.1016/j.rser.2019.05.007.
20. Tabbi Wilberforce, O. Ijaodola, Emmanuel Ogungbemi, F.N. Khatib, Zaki El-Hassan, J. Thomposon, A.G. Olabi, A comprehensive study of the effect of bipolar plate (BP) geometry design on the performance of proton exchange membrane (PEM) fuel cells, Renew. Sustain. Energy Rev. (111) (September 2019) 236–260, doi: 10.1016/j.rser.2019.04.081.
21. Tabbi Wilberforce, O. Ijaodola, Emmanuel Ogungbemi, F.N. Khatib, Zaki El-Hassan, J. Thomposon, A.G. Olabi, Numerical modelling and CFD simulation of a polymer electrolyte membrane (PEM) fuel cell flow channel using an open pore cellular foam material, Sci. Total Environ. 678 (15 August 2019) 728–740, doi: 10.1016/j.scitotenv.2019.03.430.
22. Tabbi Wilberforce, O. Ijaodola, Emmanuel Ogungbemi, F.N. Khatib, Zaki El-Hassan, J. Thomposon, A.G. Olabi, Effect of humidification of reactive gases on the performance of a proton exchange membrane fuel cell, Sci. Total Environ. 688 (20 October 2019) 1016–1035, doi: 10.1016/j.scitotenv.2019.06.397.
23. O. Ijaodola, E. Ogungbemi, F.N. Khatib, T. Wilberforce, M. Ramadan, El Hassan Z, et al., Evaluating the effect of metal bipolar plate coating on the performance of proton exchange membrane fuel cells, Energies 11 (2018), doi: 10.3390/en11113203.
24. Tabbi Wilberforce, A. Alaswad, A. Palumbo, A.G. Olabi, Advances in stationary and portable fuel cell applications, Int. J. Hydrog. Energy 41 (37) (March 2016).
25. T. Wilberforce, O. Ijaodola, E. Ogungbemi, Hassan Z El, J. Thompson, A.G Olabi, Effect of bipolar plate materials on performance of fuel cells, Ref. Modul. Mater. Sci. Mater. Eng., Elsevier (2018), doi: 10.1016/B978-0-12-803581-8.11272-X.
26. Tabbi Wilberforce, Zaki El-Hassan, F.N. Khatib, Al Makky Ahmed, Ahmad Baroutaji, James G.Carton, Abdul G. Olabi, Developments of electric cars and fuel cell hydrogen electric cars, Int. J. Hydrog. Energy 42 (40) (5 October 2017) 25695–25734, doi: 10.1016/j.ijhydene.2017.07.054.
27. T. Wilberforce, Z. El-Hassan, F.N. Khatib, A. Al Makyy, A. Baroutaji, J.G. Carton, A.G. Olabi, Modelling and simulation of proton exchange membrane fuel cell with serpentine bipolar plate using MATLAB, Int. J. Hydrog. (2017), doi: 10.1016/j.ijhydene.2017.06.091.
28. E. Ogungbemi, O. Ijaodola, F.N. Khatib, T. Wilberforce, Z. El Hassan, J. Thompson, et al., Fuel cell membranes – pros and cons, Energy (2019), doi: 10.1016/J.ENERGY.2019.01.034.
29. Tabbi Wilberforce, A.G. Olabi. Performance prediction of proton exchange membrane fuel cells (PEMFC) using adaptive neuro inference system (ANFIS). Sustainability 2020, 12, 4952; doi:10.3390/su12124952.
30. Tabbi Wilberforce, A.G. Olabi, Design of experiment (DOE) analysis of 5-cell stack fuel cell using three bipolar plate geometry design, Sustainability 12 (2020) 4488, doi: 10.3390/su12114488.